
2001

Middle-Ear Function with Tympanic-Membrane Perforations. I. Measurements and Mechanisms

Susan E. Voss
Smith College, svoss@smith.edu

John J. Rosowski
Harvard Medical School

Saumil N. Merchant
Harvard Medical School

William T. Peake
Massachusetts Eye and Ear Infirmary

Follow this and additional works at: https://scholarworks.smith.edu/egr_facpubs



Part of the [Engineering Commons](#)

Recommended Citation

Voss, Susan E.; Rosowski, John J.; Merchant, Saumil N.; and Peake, William T., "Middle-Ear Function with Tympanic-Membrane Perforations. I. Measurements and Mechanisms" (2001). Engineering: Faculty Publications, Smith College, Northampton, MA.
https://scholarworks.smith.edu/egr_facpubs/141

This Article has been accepted for inclusion in Engineering: Faculty Publications by an authorized administrator of Smith ScholarWorks. For more information, please contact scholarworks@smith.edu

Middle-ear function with tympanic-membrane perforations.

I. Measurements and mechanisms

Susan E. Voss^{a)}

Picker Engineering Program, Smith College, 51 College Lane, Northampton, Massachusetts 01063; Eaton-Peabody Laboratory of Auditory Physiology and Department of Otolaryngology, Massachusetts Eye and Ear Infirmary, Boston, Massachusetts 02114; Speech and Hearing Sciences Program, Harvard-M.I.T. Division of Health Sciences and Technology, Cambridge, Massachusetts 02139; Department of Otolaryngology, Harvard Medical School, Boston, Massachusetts; and Research Laboratory of Electronics, Massachusetts Institute of Technology, Cambridge, Massachusetts 02139

John J. Rosowski

Eaton-Peabody Laboratory of Auditory Physiology and Department of Otolaryngology, Massachusetts Eye and Ear Infirmary, Boston, Massachusetts 02114; Speech and Hearing Sciences Program, Harvard-M.I.T. Division of Health Sciences and Technology, Cambridge, Massachusetts 02139; Department of Otolaryngology, Harvard Medical School, Boston, Massachusetts; and Research Laboratory of Electronics, Massachusetts Institute of Technology, Cambridge, Massachusetts 02139

Saamil N. Merchant

Eaton-Peabody Laboratory of Auditory Physiology and Department of Otolaryngology, Massachusetts Eye and Ear Infirmary, Boston, Massachusetts 02114; Speech and Hearing Sciences Program, Harvard-M.I.T. Division of Health Sciences and Technology, Cambridge, Massachusetts 02139; and Department of Otolaryngology, Harvard Medical School, Boston, Massachusetts 02114

William T. Peake

Eaton-Peabody Laboratory of Auditory Physiology and Department of Otolaryngology, Massachusetts Eye and Ear Infirmary, Boston, Massachusetts 02114; Speech and Hearing Sciences Program, Harvard-M.I.T. Division of Health Sciences and Technology, Cambridge, Massachusetts 02139; and Department of Electrical Engineering and Computer Science and Research Laboratory of Electronics, Massachusetts Institute of Technology, Cambridge, Massachusetts 02139

(Received 27 December 2000; revised 1 March 2001; accepted 24 May 2001)

Sound transmission through ears with tympanic-membrane (TM) perforations is not well understood. Here, measurements on human-cadaver ears are reported that describe sound transmission through the middle ear with experimentally produced perforations, which range from 0.5 to 5.0 mm in diameter. Three response variables were measured with acoustic stimulation at the TM: stapes velocity, middle-ear cavity sound pressure, and acoustic impedance at the TM. The stapes-velocity measurements show that perforations cause frequency-dependent losses; at low frequencies losses are largest and increase as perforation size increases. Measurements of middle-ear cavity pressure coupled with the stapes-velocity measurements indicate that the dominant mechanism for loss with TM perforations is reduction in pressure difference across the TM; changes in TM-to-ossicular coupling generally contribute less than 5 dB to the loss. Measurements of middle-ear input impedance indicate that for low frequencies, the input impedance with a perforation approximates the impedance of the middle-ear cavity; as the perforation size increases, the similarity to the cavity's impedance extends to higher frequencies. The collection of results suggests that the effects of perforations can be represented by the path for air-volume flow from the ear canal to the middle-ear cavity. The quantitative description of perforation-induced losses may help clinicians determine, in an ear with a perforation, whether poor hearing results only from the perforation or whether other pathology should be expected. © 2001 Acoustical Society of America. [DOI: 10.1121/1.1394195]

PACS numbers: 43.64.Ha [BLM]

I. INTRODUCTION

Perforations of the tympanic membrane (TM) can result from trauma, middle-ear disease, or the treatment of middle-ear disease. Perforations occur as a result of the disease pro-

cess in chronic otitis media, which affects at least 0.5% of the population (Sadé, 1982). Additionally, it is estimated that 1.3% of American children have tympanostomy tubes (Bright *et al.*, 1993), which are tubes placed in the TM that, like a perforation, connect the ear canal to the middle-ear cavity. Although TM perforations occur frequently, their effects on hearing are uncertain: "There is no general agreement among clinicians about the magnitude and the configu-

^{a)}Author to whom correspondence should be addressed. Address for correspondence: Smith College, Picker Engineering Program, 51 College Lane, Northampton, MA 01063; electronic mail: svoss@email.smith.edu

ration of the hearing loss that is caused by various types of tympanic-membrane perforations” (Terkildsen, 1976). This paper, along with the theoretical companion paper (Voss *et al.*, 2001d), provides controlled measurements together with a theory for middle-ear function with perforations. Results from both papers will be important in the future design of controlled clinical experimental studies.

To determine the effects of perforations, we have made measurements on human cadaveric temporal-bone preparations with controlled perforations in otherwise normal ears. The work reported here is organized both (1) to describe how perforations alter middle-ear function from normal and (2) to determine the relative importance of particular mechanisms that contribute to hearing loss with perforations. The companion paper (Voss *et al.*, 2001d) uses these experimental results to develop a mathematical model of sound transmission with perforations.

We present measurements of several acoustic quantities with perforations. The ratio between the stapes velocity (V_S) and the sound pressure in the ear canal at the TM (P_{TM}) is our measure of middle-ear sound transmission to the cochlea, i.e.,

$$T \equiv \frac{V_S}{P_{TM}} \equiv \text{middle-ear transmission.} \quad (1)$$

Perforations of the TM may change middle-ear sound transmission through at least three mechanisms.

(1) Perforations may alter the pressure difference across the TM, which drives the motion of the TM and ossicular chain, and thereby change ossicular motion (e.g., Mehmke, 1962; McArdle and Tonndorf, 1968; and Kruger and Tonndorf, 1977, 1978).

(2) Perforations may alter the coupling between the pressure difference across the TM and the malleus motion, thereby changing ossicular motion. Specific suggestions that fall in this category include (a) decrease in the effective TM area (e.g., Austin, 1978; Shambaugh, 1967), (b) change in the coupling between TM motion and malleus motion, and (c) change in tension of the TM that results from disruption of its fibrous structure (Lim, 1970).

(3) Perforations may alter the sound pressures that act directly on the oval and round windows (e.g., Shambaugh, 1967; Hughes and Nodar, 1985, p. 72; Schuknecht, 1993b, p. 196), thereby changing the pressure difference between the windows, which is a component of the stimulus to the cochlea (Voss *et al.*, 1996).

Measurements reported here determine the relative importance of mechanisms (1) and (2) above; we have shown elsewhere that mechanism (3) is not an important route of sound transmission with most perforations (Voss 1998, Chap. 3). To separate the effects of mechanisms (1) and (2), we use measurements of stapes velocity (V_S), pressure at the TM (P_{TM}), and middle-ear cavity pressure (P_{cav}), to define two ratios,

$$H_{\Delta TM} \equiv \frac{P_{TM} - P_{cav}}{P_{TM}} \equiv \text{pressure-difference ratio,} \quad (2)$$

and

$$H_{TOC} \equiv \frac{V_S}{P_{TM} - P_{cav}} \equiv \text{TM coupling ratio.} \quad (3)$$

[The subscript TOC stands for TM–ossicles–cochlea.] H_{TOC} is a measure of sound transmission through the TM and ossicular chain that eliminates the effects of changes in pressure difference across the TM.

The product of the two ratios is middle-ear transmission T , i.e.,

$$T \equiv \frac{V_S}{P_{TM}} = \underbrace{\frac{P_{TM} - P_{cav}}{P_{TM}}}_{H_{\Delta TM}} \underbrace{\frac{V_S}{P_{TM} - P_{cav}}}_{H_{TOC}}. \quad (4)$$

Changes in the factors, $H_{\Delta TM}$ and H_{TOC} , provide measures of the importance of mechanisms (1) and (2) in determining transmission loss with perforations. As we will see, perforation-induced changes in transmission (i.e., changes in V_S/P_{TM}) result primarily from one of these mechanisms.

In addition to measurements of the quantities in Eq. (4), we also present measurements of the impedance at the TM (Z_{TM}). These impedance measurements are critical in defining a model of the middle ear with a perforation (Voss *et al.*, 2001d), and they also allow estimation of the effects of perforations on the sound pressure generated at the TM by audiologic earphones (Voss *et al.*, 2000a, e).

II. METHODS

A. Temporal bones and their preparation

Acoustic measurements of stapes velocity, middle-ear cavity pressure, and impedance in the ear canal near the tympanic membrane (TM) were made in cadaveric temporal bones with both normal and perforated TMs. The subjects were 11 of the ears for which normal results are presented in Voss *et al.* (2000b), where measurement techniques are described in detail. Measurements are reported from 100 to 4000 Hz, as some measurements above 4000 Hz were in the noise floor.

Measurements were made on fresh temporal bones for which no evidence of otologic disease was found either in medical records or in oto-microscopic examination. In each temporal bone, the ear canal was drilled away to expose the TM, and a brass ring was cemented to the bony rim around the TM to allow repeatable coupling to the sound source. Access to the stapes footplate was obtained by opening the “facial recess” from a posterior-tympanotomy approach (e.g., Shambaugh and Glasscock, 1980, pp. 704–705). To increase visibility of the stapes, (1) the stapedius tendon was cut with alligator-type surgical scissors, (2) the pyramidal process was curetted away, and (3) the mastoid segment of the facial nerve was removed. A 0.25 mm² piece of reflective tape, coated with 50 μm polystyrene spheres packed side by side and weighing 0.05 mg, was placed on either the stapes footplate or the posterior crust of the stapes. Voss *et al.* (2000b) and Voss (1998) illustrate the (minimal) effects of these manipulations on the measured stapes velocity. The middle-ear cavity pressure was measured adjacent to the stapes via a probe tube that was cemented to the temporal

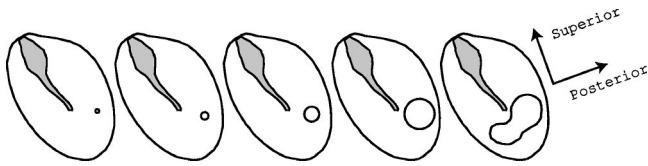


FIG. 1. Schematic drawing of the TM and the manubrium of the malleus that illustrates how perforations of increasing size were made. The diameters for the illustrated circular perforations are, from left to right, 0.5, 1, 2, and 4 mm.

bone and terminated by a calibrated microphone. Measurements were made with the middle-ear cavity closed. Periodically during the measurement sessions, the bone was submerged in normal saline for several seconds, and the excess fluid removed with gentle suction.

B. Perforation of the tympanic membrane

In each ear, perforations of different sizes and locations were made. Typically, increasing-sized circular perforations were made in the pars tensa in either the posterior-inferior (PI) or the anterior-inferior (AI) quadrant. In most cases, once an entire quadrant was perforated, a kidney-shaped perforation that included both inferior quadrants was made so that most of the inferior half of the TM was removed. A typical sequence of perforations is illustrated in Fig. 1.

The controlled perforations were made with an otosurgical Argon laser (i.e., an HGM, Inc. laser used at a power level of 1–2 mW and pulse duration of 100 ms). In order to measure the perforation sizes, an image of the TM was video taped as each perforation was made, and a scale was placed next to the perforation. Later, the video tape was viewed with a video monitor and the perforation was traced and measured to obtain its area. We report a diameter calculated from the area measurement for each perforation. For kidney-shaped perforations that involve more than one quadrant, we report the diameter of a circular perforation of the same area.

C. Calculation of pressure at the tympanic membrane

We measured the ear-canal sound pressure about 3 mm lateral to the TM, as described in detail in Voss *et al.* (2000b) and Voss (1998). To correct for differences in pressure between this location and the TM we use a lossless cylindrical-tube model to represent the residual ear-canal air space (e.g., Møller, 1965; Rabinowitz, 1981; Lynch *et al.*, 1994; Huang *et al.*, 1997), and we estimate the pressure P_{TM} at the TM as

$$P_{TM} = \frac{P_{EC} Z_{TM}}{Z_{TM} \cos(kl) + jZ_0 \sin(kl)}, \quad (5)$$

where P_{EC} is the measured pressure at the microphone probe-tube orifice; Z_{TM} is the measured impedance at the TM (see Sec. II G); $Z_0 = \rho c/A$ is the characteristic impedance of the tube, and $A = 70 \text{ mm}^2$ is the area of the tube which is defined by the average area of the TM (Wever and Lawrence, 1954, p. 416); l is the length of the tube and is defined as $l = V_{EC}/A$, where V_{EC} is the ear-canal air volume between the microphone probe-tube orifice and the TM, which is measured by filling the residual ear-canal air space with saline using a calibrated syringe (range 0.03–0.1 cm^3); k

$= 2\pi f/c$, ρ is the density of air, c is the velocity of sound in air, and f is frequency.

The ratio P_{TM}/P_{EC} is less than 1 dB in magnitude and only a few hundredths of a cycle in angle for perforations that are less than 1 mm in diameter. At the other extreme, when the TM is entirely removed, the ratio P_{TM}/P_{EC} can approach ± 2 dB in magnitude and 0.05 cycles in angle for frequencies above 1000 Hz. Below 1000 Hz, the differences between P_{EC} and P_{TM} are smaller than 1 dB for all TM conditions.

In this paper, we apply the sound-pressure correction of Eq. (5) to convert measurements of P_{EC} to P_{TM} . However, as measurements of Z_{TM} were not obtained on one ear (bone 18), we use P_{EC} for all results on bone 18.

D. Measurement of the stapes velocity

1. Scope

We use our measurements of T (i.e., V_S/P_{TM}) as a description of the sound transmission through the middle ear. Our techniques are described in Voss *et al.* (2000b) and Voss (1998). Specifics relevant to the measurements with perforations are presented here.

2. Acoustic stimuli

Unless otherwise noted, the measurements of stapes velocity were made in response to tonal stimuli that were typically between 90 and 120 dB SPL. [The system behaved linearly for these levels, as described by Voss *et al.* (2000b).] For each tone, the two responses, ear-canal pressure and stapes velocity, were typically the average of 1000 or 2000 41-ms-long responses for a total of 41 or 82 s of averaging. The measured frequency range was 25 to 10 000 Hz; the frequency resolution was not identical for all experiments. Because the experiments on the first three ears had a poor frequency resolution (only 16 or 25 logarithmically spaced points), the reported means include only the experiments on the final eight ears, which had 68 logarithmically spaced points. [In all cases, data from the first three ears are consistent with those from the final eight ears.]

3. Removal of data affected by the mechanical artifact

Our stapes-velocity measurements are affected by a mechanical artifact, which appears to result from vibration of the sound source. This artifact confounds the measurement of stapes velocity. We measured the artifact as the velocity of the temporal bone (at the round-window niche) in response to sound in the ear canal. Specifically, we placed a piece of reflective tape on the bony round-window niche and measured the ratio between this temporal-bone velocity and the ear-canal pressure, V_{bone}/P_{TM} . With a normal TM, $|V_{bone}/P_{TM}|$ was usually more than 20 dB smaller than $|V_S/P_{TM}|$, and therefore the artifact was negligible. However, as perforations were made, the stapes velocity decreased for a constant pressure at the TM, and the mechanical artifact could interfere with measurement of the stapes velocity. Unless noted, data corresponding to stapes-velocity

magnitudes within 20 dB of the artifact magnitude $|V_{\text{bone}}/P_{\text{TM}}|$ are not included. Further details are in Voss (1998, pp. 34–35, Fig. 1–5).

The requirement that the stapes-velocity magnitude be at least 20 dB greater than the artifact's magnitude has the effect of eliminating data in which the stapes-velocity magnitude is smallest, i.e., at the lowest frequencies with the largest perforations.

4. Definition of transmission loss

To describe sound transmission with perforations, we compare the transmission measured with an intact TM, T^{norm} [i.e., $(V_S/P_{\text{TM}})^{\text{norm}}$], to the same ratio measured with a perforated TM, T^{perf} . The ratio between the normal and the perforated condition serves as our measure of transmission loss

$$\Delta T \equiv \frac{T^{\text{norm}}}{T^{\text{perf}}} \equiv \frac{(V_S/P_{\text{TM}})^{\text{norm}}}{(V_S/P_{\text{TM}})^{\text{perf}}} \equiv \text{transmission loss.} \quad (6)$$

E. Pressure-difference ratio, $H_{\Delta\text{TM}}$

1. Calculation of the pressure-difference ratio

We calculate the pressure difference across the TM from measurements of ear-canal pressure and middle-ear cavity pressure. The ear-canal pressure, P_{EC} , is generated and measured with the acoustic assembly described by Voss *et al.* (2000b), and P_{TM} is computed from P_{EC} via Eq. (5). The middle-ear cavity pressure, P_{cav} , is measured with a probe-tube microphone that is placed near the stapes footplate within the middle-ear cavity. Details of this probe-tube microphone and its calibration are in Voss *et al.* (2000b). We compute $H_{\Delta\text{TM}}$, the pressure-difference ratio, as

$$H_{\Delta\text{TM}} \equiv \frac{\Delta P_{\text{TM}}}{P_{\text{TM}}} \equiv \frac{P_{\text{TM}} - P_{\text{cav}}}{P_{\text{TM}}}. \quad (7)$$

To describe how perforations affect $H_{\Delta\text{TM}}$, we compute changes in $H_{\Delta\text{TM}}$ for the intact TM relative to the perforated TM as

$$\Delta H_{\Delta\text{TM}} \equiv \frac{H_{\Delta\text{TM}}^{\text{norm}}}{H_{\Delta\text{TM}}^{\text{perf}}} \equiv \text{change in } H_{\Delta\text{TM}}. \quad (8)$$

2. Limits on the accuracy of pressure-difference calculations

With the TM perforated, the middle-ear cavity pressure and the pressure at the TM are nearly equal at low frequencies. Thus, small errors in the relative calibration of the two microphones that measure these two pressures may introduce large errors in the computed pressure difference. The calibration procedure for the microphone that measures P_{cav} is described by Voss *et al.* (2000b). This microphone is calibrated relative to the microphone that measures P_{EC} by acoustically coupling the two microphones together and comparing their responses to the common stimulus. To estimate the variability in the relative calibrations between the two microphones, we examined repeated relative calibrations over the course of a single experiment. In general, the ratio between repeated calibrations during an experiment varied as much as a factor

of 1.1 in magnitude and 0.01 cycles in angle. With such an error and with P_{cav} equal to P_{TM} , a measurement would yield

$$|H_{\Delta\text{TM}}| = \left| \frac{P_{\text{TM}} - 1.1P_{\text{TM}}e^{j2\pi 0.01}}{P_{\text{TM}}} \right| = 0.12, \quad (9)$$

although $H_{\Delta\text{TM}}$ would really be zero. Thus, measured $|H_{\Delta\text{TM}}|$ values of less than 0.12 may be highly affected by calibration errors. Thus, we impose the lower limit of 0.12 on the magnitude of the pressure-difference ratio ($|H_{\Delta\text{TM}}|$) computed from Eq. (7), and any calculated $|H_{\Delta\text{TM}}|$ that is below 0.12 is eliminated from the results.

3. Acoustic stimuli for cavity-pressure measurements

The voltages that correspond to the pressures P_{EC} and P_{cav} are measured simultaneously on two channels in response to a chirp stimulus. The chirp contains 1024 linearly spaced frequencies from 24 to 25 000 Hz. The reported response is the average of 200 responses (8.2 s of averaging).

F. TM coupling ratio, H_{TOC}

Perforation-induced changes in H_{TOC} are a measure of sound transmission through the TM and ossicular chain that eliminates the effects of changes in pressure differences across the TM with different perforations. H_{TOC} is calculated from measurements as

$$H_{\text{TOC}} \equiv \frac{V_S/P_{\text{TM}}}{(P_{\text{TM}} - P_{\text{cav}})/P_{\text{TM}}} \equiv \frac{V_S/P_{\text{TM}}}{H_{\Delta\text{TM}}}. \quad (10)$$

Changes in H_{TOC} are calculated as the ratio of the normal $H_{\text{TOC}}^{\text{norm}}$ to the perforated $H_{\text{TOC}}^{\text{perf}}$.

$$\Delta H_{\text{TOC}} \equiv \frac{H_{\text{TOC}}^{\text{norm}}}{H_{\text{TOC}}^{\text{perf}}} \equiv \text{change in } H_{\text{TOC}}. \quad (11)$$

To calculate H_{TOC} [Eq. (10)], some data manipulation was required. The measurements of V_S/P_{TM} were made with a frequency resolution of 68 points from 24 to 10 000 Hz, whereas the measurements of $H_{\Delta\text{TM}} = \Delta P_{\text{TM}}/P_{\text{TM}}$ [Eq. (7)] were made with a frequency resolution of 1024 points from 24 to 25 000 Hz. Thus, the two kinds of measurements are not at exactly the same frequencies. We resolved this problem through interpolation of the $H_{\Delta\text{TM}}$ data to the frequencies of the V_S/P_{TM} data, where the $H_{\Delta\text{TM}}$ data have the larger frequency resolution of the two measurements. Interpolation is done using cubic spline interpolation performed using the software package MATLAB (The Mathworks, Inc.). Note that the displayed H_{TOC} 's do not include points where either (1) $|V_S/P_{\text{TM}}|$ is within 20 dB of the mechanical artifact or (2) $|H_{\Delta\text{TM}}| < 0.12$.

G. Measurement of the middle-ear input impedance

Acoustic impedance measurements were made with a method similar to that used by others (e.g., Rabinowitz, 1981; Allen, 1986; Lynch *et al.*, 1994), which is thoroughly discussed elsewhere (Voss, 1998; Voss *et al.*, 2000b). The Thévenin equivalent of the sound-delivery system was determined by pressure measurements in two "reference loads" of known theoretical impedance. The two theoretical imped-

ances were calculated from the equations of Egolf (1977) and combined with the pressure measurements made in the two reference loads to calculate the source's Thévenin pressure and impedance equivalents P_{TH} and Z_{TH} . The ear's impedance was then calculated from a pressure measurement in response to a chirp stimulus in the ear canal. The impedance measurements were estimated to be generally accurate to within about 10% in magnitude (about 1 dB) and 10° in angle (0.025 cycles).

Impedances were measured with a different acoustic assembly from that used for the stapes-velocity and the middle-ear cavity pressure measurements. (The source used for the stapes-velocity and middle-ear cavity pressure measurements had a source impedance magnitude that was small compared to the magnitude of the input impedance of the middle ear; thus, it could not be used to make accurate impedance measurements.) The impedance-measurement assembly consisted of a Knowles ED-1913 hearing aid receiver as a sound source (Knowles Electronics, Elk Grove, IL) and a Knowles EK-3027 microphone (Ravicz *et al.*, 1992; Voss, 1998). (The source used to measure impedance in the ear canal was not useful for the stapes velocity measurements because it could not generate large enough sound-pressure levels in all situations.)

The ear's impedance was measured in the ear canal (1) with an intact TM, (2) after each perforation was made (Z_{TM}^{perf}), and (3) with the TM removed. The impedance measurement was made at the same ear-canal location as the ear-canal pressure (Sec. II C), and we approximate the effect of the ear-canal air volume on the measured impedances by a lossless cylindrical-tube model of the residual ear-canal air space (e.g., Møller, 1965; Rabinowitz, 1981; Lynch *et al.*, 1994; Huang *et al.*, 1997), so that the impedance at the TM (Z_{TM}) is determined from the impedance measured in the ear canal Z_{EC} as

$$Z_{TM} \equiv Z_0 \frac{Z_{EC} - jZ_0 \tan(kl)}{Z_0 - jZ_{EC} \tan(kl)}, \quad (12)$$

where the variables in Eq. (12) are defined in conjunction with Eq. (5).

With an intact TM, the ratio $|Z_{EC}/Z_{TM}|$ approaches -3 dB with the largest ear-canal volume of 0.1 cm^3 ; in cases with smaller ear-canal air volumes, $|Z_{EC}/Z_{TM}|$ is between 0 and -1 dB. With perforations, the ratio $|Z_{EC}/Z_{TM}|$ can approach 3 dB for frequencies near 2000–4000 Hz.

III. RESULTS

A. Organization

The results are organized into five sections. Each of the first four sections focuses on one of the four measured ratios for a series of perforations: (1) middle-ear transmission $T \equiv V_S/P_{TM}$; (2) the pressure-difference ratio $H_{\Delta TM}$; (3) the TM coupling ratio H_{TOC} ; and (4) the middle-ear input impedance Z_{TM} . In each section, we show data from a typical "example" ear (bone 24L). Additionally, we show the means from eight ears for the quantities ΔT , $\Delta H_{\Delta TM}$, and ΔH_{TOC} . In all cases, results from the example ear are similar to those from the other ears, which are plotted in the appendices of

Voss (1998). Measurements were made on eleven ears. However, measurements on the first three ears had poor frequency resolution (only 16 or 25 logarithmically spaced points) whereas the experiments on the final eight ears had a frequency resolution of 68 logarithmically spaced points. For this reason, the reported means include only the final eight experiments. In all cases, data from the first three ears are consistent with those from the final eight ears.

A basic conclusion supported by the results is that the effects of perforations on sound transmission result primarily from perforation-induced changes in the pressure difference across the TM, with alterations in TM-to-ossicular-coupling (H_{TOC}) being relatively small. One experiment, reported in Sec. III F, was designed to determine what modifications in the TM are required to make major changes in this coupling; this experiment determined the effects of extensive slits in the TM on H_{TOC} .

B. Middle-ear transmission T

1. Components of stapes motion

Voss *et al.* (2000b) show that the stapes translates in and out of the oval window with a piston-like motion for frequencies up to at least 2000 Hz when the TM is normal. Voss *et al.* (2000b) argue that to be consistent with translational motion, the ratio between the velocities measured at two locations on the stapes has to (1) have a magnitude that is constant versus frequency, and (2) have an angle that is zero. To determine whether the stapes motion is piston-like when the TM is perforated, stapes-velocity measurements at two stapes locations were made on two ears with perforations [two of the five ears in Fig. 6 of Voss *et al.* (2000b)]. For each perforation condition, the ratio of the complex velocities measured at two locations was computed. In Fig. 2, the magnitudes and angles of the velocity ratios associated with these two ears are plotted for four perforation sizes. Below 2000 Hz, the magnitudes and angles with the perforations appear similar to those shown for the normal TM: the magnitudes are nearly constant and the angles are near zero, consistent with a translational motion. Above 2000 Hz, there is more variability in both the magnitudes and angles, which might result from a more complicated motion. However, moderate changes in the preparation between measurements could produce the differences seen in Bone 29. In neither ear do the changes have a systematic dependence on perforation size, which is consistent with another source for the change. In summary, up to at least 2000 Hz, the stapes appears to move with a one-dimensional translational motion with both a normal and a perforated TM.

2. Effects of perforations on transmission

a. Example ear. Measurements of middle-ear transmission T (i.e., V_S/P_{TM}) from the example ear are shown as a function of frequency with perforation diameter as a parameter in Fig. 3 (left). The magnitude and angle of T have several features that are consistent across all preparations. First consider the magnitude $|T|$: (1) As perforation diameter increases, $|T^{perf}|$ decreases systematically at frequencies below 1000–2000 Hz; (2) at frequencies less than 1000 Hz, for all perforation diameters, $|T^{perf}|$ increases with increasing

Stapes motion: Pure translation?

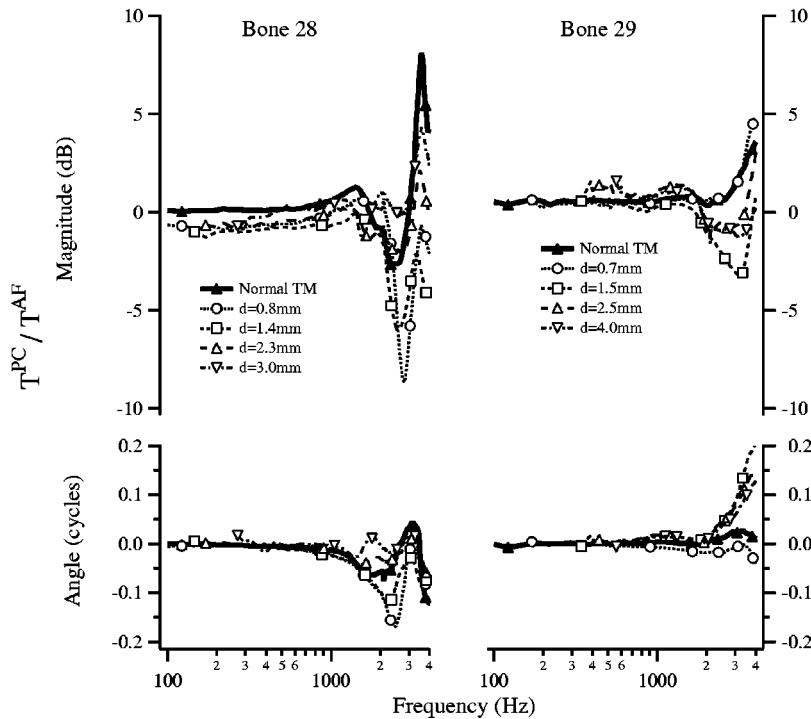


FIG. 2. Magnitude and angle of ratio of stapes velocities measured at two locations on the stapes. $T \equiv V_S / P_{TM}$ was measured at two locations on the stapes of bones 28 and 29 with the TM both normal and perforated. For both bones, the measurement locations were the anterior end of the stapes footplate (AF) and the posterior crus (PC). Thus, for each TM condition noted in the legends, “Magnitude (dB)” refers to $20 \log_{10} |T^{PC}/T^{AF}|$, and “Angle” refers to the difference $\angle(T^{PC}) - \angle(T^{AF})$. The middle-ear cavities were open for the measurements on bone 28 and sealed for the measurements on bone 29. Measurement stimuli were chirps, and symbols that distinguish between measurements are plotted at every 30th data point.

frequency such that in the 1000 Hz range $|T^{perf}|$ approaches the normal value, and in many cases $|T^{perf}|$ exceeds $|T^{norm}|$ slightly; and (3) above 1000 Hz, the perforations’ effects are generally smaller than at frequencies below 1000 Hz.

Next, consider the angle $\angle T$. With the TM intact, $\angle T^{norm}$ is constant at about 0.25 cycles at frequencies up to

at least 500 Hz, and above about 500 Hz, $\angle T^{norm}$ decreases gradually with increasing frequency. When the TM is perforated: (1) At low frequencies, $\angle T^{perf}$ is roughly constant with frequency but its low-frequency asymptote appears to be between 0.25 and 0.75 cycles. Larger perforations result in larger low-frequency angles; and (2) as frequency increases,

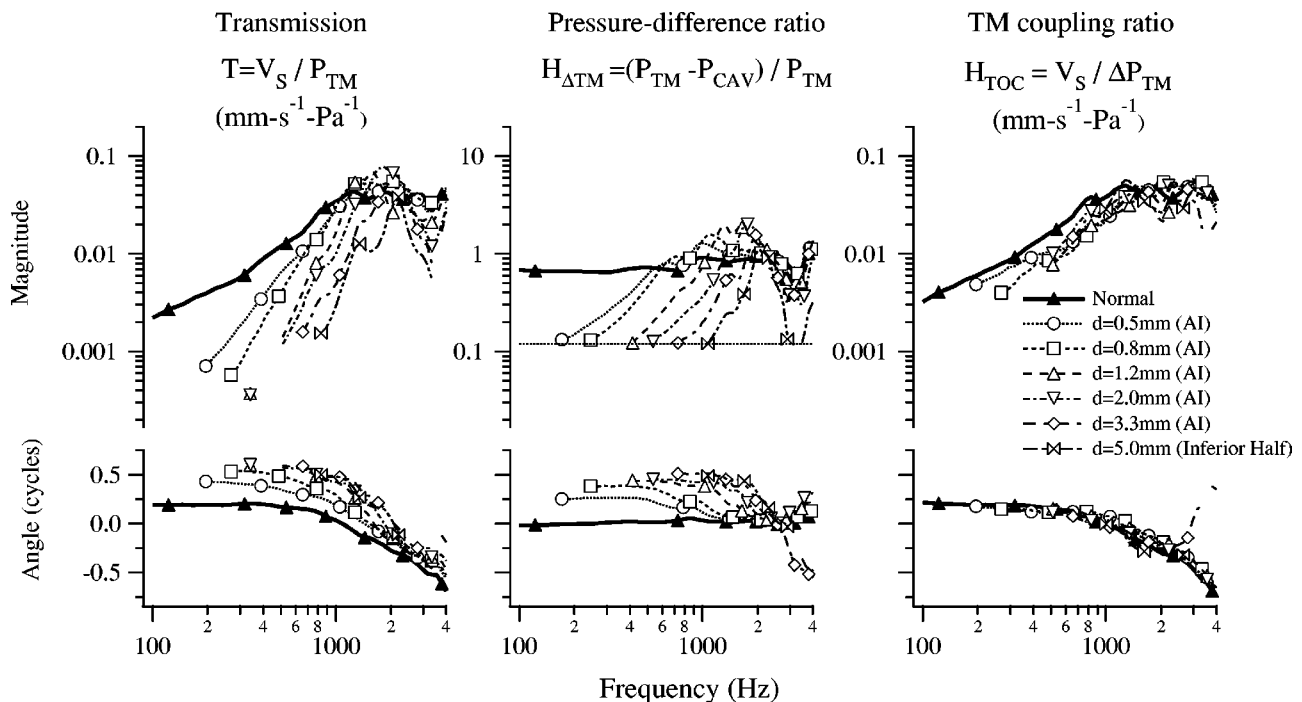


FIG. 3. Measurements of T (left), $H_{\Delta TM}$ (center), and H_{TOC} (right) from the example ear (Bone 24L). For each quantity, the magnitude (upper) and angle (lower) of each measurement are plotted. The legend in the rightmost panel specifies the perforation diameter. The smaller perforations were in the anterior-inferior (AI) quadrant, and the largest perforation contained most of the inferior half of the TM. Symbols are plotted at every eighth data point for T and H_{TOC} and every 25th data point for $H_{\Delta TM}$. “Gaps” between T data points result when measurements at some frequencies are excluded by the mechanical artifact criterion. The horizontal dashed line in $|H_{\Delta TM}|$ indicates a pressure difference of 0.12, which is the lower limit for the calculated $|H_{\Delta TM}|$.

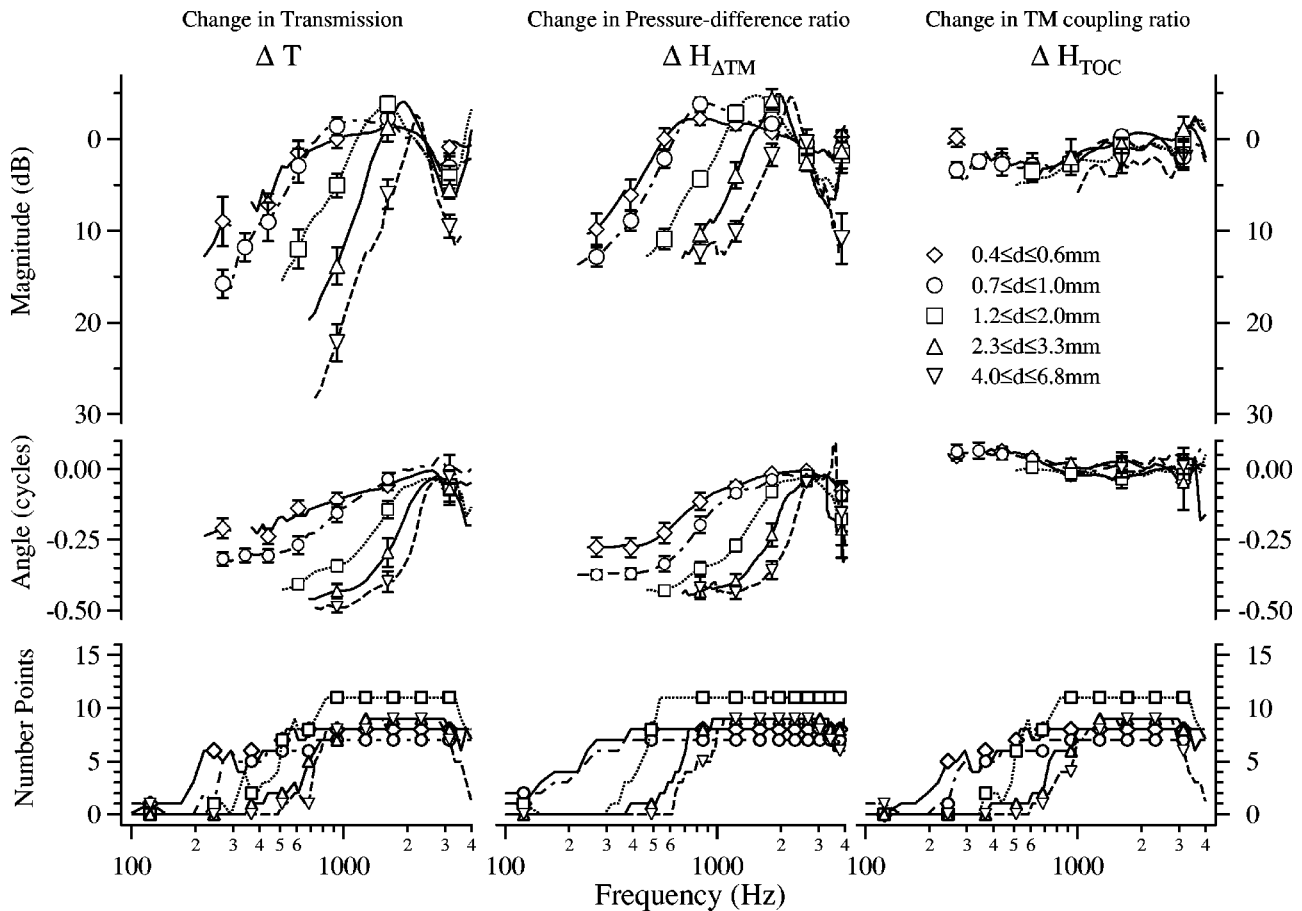


FIG. 4. Mean change (\pm standard error) in T (left), $H_{\Delta TM}$ (center), and H_{TOC} with perforation diameter as a parameter; the changes from normal are defined as the ratio between the normal measurement and the perforated measurement (i.e., norm/perf), with |norm/perf| plotted in dB with positive down so that these plots have the format of standard audiograms. Mean magnitudes (upper) were calculated in the logarithmic domain, and mean angles (middle) in the linear domain. Changes from all perforations are included from the final eight experiments. Each change curve, with diameter as a parameter, includes all perforations made on the eight ears that fit the diameter category. The lower plots indicate the total number of measurements in each diameter category that are available at each frequency: N is not constant across frequency because points where either V_S/P_{TM} is within 20 dB of the artifact or where $|H_{\Delta TM} < 0.12|$ are not included in calculation of the means. Means are only calculated at frequencies where data from more than 50% of the cases in the range category are above our noise limits. To increase visibility, symbols and standard error bars are indicated at a subset of data points.

$\angle T^{perf}$ decreases and approaches the value for the intact TM $\angle T^{norm}$.

b. Means from eight ears. In this section, we compare the effects of perforations on T for measurements made on eight ears. In order to compare the effect of the perforation across different ears that vary in their baseline (i.e., intact TM) responses, we compare changes from normal in stapes velocity [i.e., ΔT of Eq. (6)].

A total of 44 perforations were made on the eight ears. To compare the effects of all 44 perforations, we grouped the perforations by size. Diameter categories were selected by grouping the 44 perforations into 5 categories so that (1) there were approximately the same number in each group (range 7–11) (Fig. 4 lower-left), (2) the ratio of the maximum-to-minimum perforation diameter in each group is similar for all groups (range 1.4–1.7), and (3) gaps between groups are similar across all five groups (15%–20%).

The mean perforation-induced changes from the intact condition (i.e., transmission loss) are plotted in Fig. 4 (left-hand side). The mean changes in transmission, ΔT , are consistent with the features described above for the measurements from the example ear: (1) ΔT is frequency dependent

with the largest reductions in magnitude occurring at low frequencies; (2) at low frequencies, ΔT increases with perforation size; (3) between 1000 and 2000 Hz, there can be small increases (i.e., 3 dB) in ΔT with perforations; both the frequency and the sharpness of this peak increase with perforation-diameter increases; (4) from about 2000 to 4000 Hz, changes are less than 12 dB and increase with perforation size; and (5) for the lowest frequencies the mean angle change approaches -0.25 cycles for the smallest perforations and -0.5 cycles for the larger perforations; for the middle frequencies the angle changes are near zero, and for the higher frequencies the mean angle changes are between zero and -0.25 cycles.

C. Pressure-difference ratio: $H_{\Delta TM}$

Measurements of the pressure-difference ratio $H_{\Delta TM}$ from the example ear are shown as a function of frequency with perforation diameter as a parameter in Fig. 3 (center). With the TM intact, the magnitude ranges from about 0.7 to 1 and is nearly independent of frequency; the angle is about zero. Perforations have their biggest effects on $H_{\Delta TM}$ at fre-

quencies below about 1000 Hz, where many of the effects are similar to those described previously for T . For example: (1) the low-frequency magnitude $|H_{\Delta\text{TM}}|$ decreases systematically as perforation diameter increases and (2) $|H_{\Delta\text{TM}}|$ has a maximum where the “perforated” measurement exceeds the normal measurement, and the frequency of this maximum increases with perforation diameter. At the frequency of the maximum, the angle $\angle H_{\Delta\text{TM}}$ begins to decrease toward 0 cycles: For the smallest perforation this angle decrease is about 0.25 cycles and for the largest perforations the angle decrease approaches 0.5 cycles. For the larger perforations, the combination of the magnitude maximum and the half-cycle angle change suggests that the perforation introduces a resonance—which might involve the effective mass of the perforation and the compliance of the middle-ear cavity (Voss *et al.*, 2001d).

Figure 4 (center) plots the mean changes from normal in $H_{\Delta\text{TM}}$ [i.e., $\Delta H_{\Delta\text{TM}}$ of Eq. (8)]. Both the magnitude and the angle of the changes from normal are similar to the measurements of $H_{\Delta\text{TM}}$ (Fig. 3 center) because with a normal TM $H_{\Delta\text{TM}}$ is nearly one in magnitude and zero in angle.

D. TM coupling ratio: H_{TOC}

The TM coupling ratio is a measure of signal transmission coupled by the TM and ossicular chain with the effects of perforations on the pressure difference across the TM removed. H_{TOC} with an intact TM is roughly the same as the transmission T with an intact TM (Fig. 3) because $|P_{\text{cav}}| < 0.3|P_{\text{TM}}|$. Perforations have only moderate effects on H_{TOC} (Fig. 3 right and Fig. 4 right). With all perforations, the changes from normal in H_{TOC} are generally less than 5 dB in magnitude and less than 0.1 cycles in angle for all frequencies. These changes are small compared to the changes in T and $H_{\Delta\text{TM}}$. Thus, changes in transmission T appear to result primarily from changes in the pressure difference across the TM, with smaller changes in the way the TM couples to the cochlea. We address this finding further in Sec. III F. [One limitation on this description results from the lack of measurements of either stapes velocity or pressure difference across the tympanic membrane at the lowest frequencies for the larger perforations, as measurements of V_S were limited at the lowest frequencies by the mechanical artifact and measurements of ΔP_{TM} with perforations yielded low-frequency pressure differences that were too small to measure accurately.]

E. Impedance at the tympanic membrane: Z_{TM}

In Fig. 5, measurements of the acoustic impedance at the TM [Eq. (12)] are plotted for our example ear with a normal ($Z_{\text{TM}}^{\text{norm}}$), perforated ($Z_{\text{TM}}^{\text{perf}}$), and removed TM (Z_{cav}). Below 500 Hz, Z_{TM} is compliance-like for all conditions, i.e., the slope of the magnitude $|Z_{\text{TM}}|$ approximates -20 dB/decade, and the low-frequency angle of $\angle Z_{\text{TM}}$ is near -0.20 cycles.

First, consider the perforation’s effect on the impedance magnitude. At the lower frequencies, a perforation reduces $|Z_{\text{TM}}^{\text{norm}}|$ by a constant, frequency-independent factor of about 0.3. This reduction is independent of perforation diameter. Above about 500 Hz, $|Z_{\text{TM}}^{\text{perf}}|$ shows perforation-diameter de-

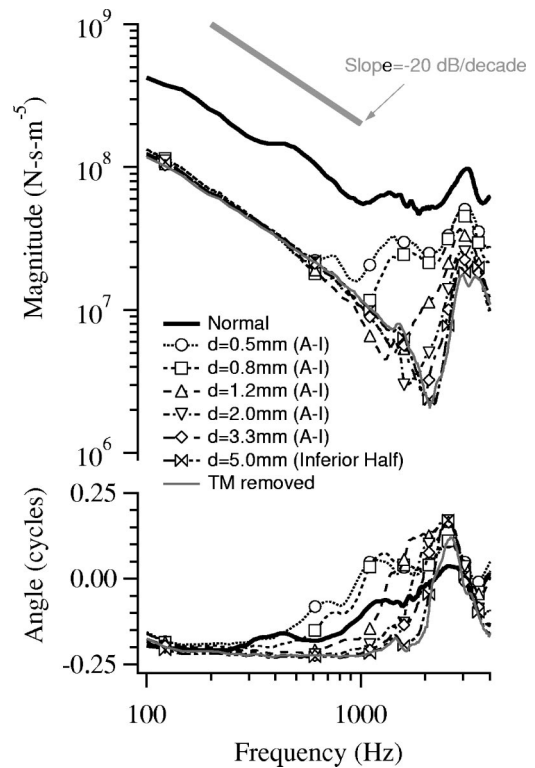


FIG. 5. Impedances at the TM measured on the example ear (bone 24 Left) for the normal TM ($Z_{\text{TM}}^{\text{norm}}$), perforated TM ($Z_{\text{TM}}^{\text{perf}}$), and TM removed (Z_{cav}) conditions. Symbols indicate every 20th data point. Upper: magnitude, lower: angle.

pendent variations. First, $|Z_{\text{TM}}^{\text{perf}}|$ has a well-defined local minimum that depends on diameter in a systematic way; as perforation diameter increases, the frequency of the minimum increases, the magnitude at the minimum frequency decreases, and the sharpness of the minimum increases. Second, $|Z_{\text{TM}}^{\text{perf}}|$ has a well-defined local maximum around 3000 Hz; the frequency of this maximum is not affected by the perforation diameter and the magnitude of the maximum decreases as perforation diameter increases.

Perforations also affect the angle of the impedance. At low frequencies, the compliant-like angle approximates -0.20 cycles for both the normal and the perforated conditions. As frequency increases, the angle increases to a positive value between 0 and 0.25 cycles. With the moderate- and larger-sized perforations, the increase in angle occurs across the same frequency range as the first local minimum in magnitude described previously. As perforation diameter increases, the transition frequency from compliant-like to resistive and mass-like increases. Around 3000 Hz, corresponding to the local magnitude maximum described previously, $\angle Z_{\text{TM}}^{\text{perf}}$ decreases.

The measurements of the impedance with the TM removed (designated as Z_{cav}) are included in Fig. 5. Comparison of the measurements of $Z_{\text{TM}}^{\text{perf}}$ to Z_{cav} indicate that (1) at the lowest frequencies $Z_{\text{TM}}^{\text{perf}} \approx Z_{\text{cav}}$ for all perforation sizes, and (2) at higher frequencies, as the perforation diameter increases, $Z_{\text{TM}}^{\text{perf}}$ approaches Z_{cav} .

The regular occurrence of a minimum in $|Z_{\text{TM}}|$ (Fig. 5) at a frequency where the angle changes rapidly, suggests a

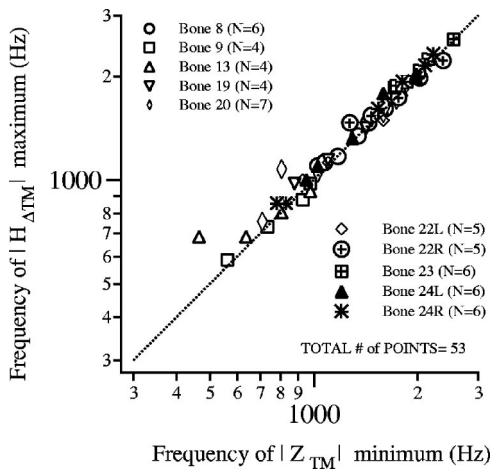


FIG. 6. Comparison of frequencies of the first maximum in $|H_{\Delta TM}|$ to frequencies of the first minimum in $|Z_{TM}|$ for 53 pairs of measurements with perforations (in 10 ears). A symbol is plotted for each perforation including the condition of TM removed. The dotted line is $y=x$.

perforation-dependent resonance involving the acoustic mass of the perforation and the acoustic compliance of the middle-ear cavity. In this case, at the resonant frequency, the pressure difference across the TM should be a maximum [Voss *et al.*, 2001d, Eq. (3)]. This prediction can be tested by comparing the frequencies of the minima of $|Z_{TM}|$ to those of the

maxima of $|H_{\Delta TM}|$. Figure 6 shows that these two independent sets of measurements fit this prediction.

F. Effects of slit-like perforations

The results presented previously indicate that even large perforations produce relatively small (i.e., less than 10 dB) changes in the coupling of pressure difference across the TM to the ossicles and cochlea (i.e., ΔH_{TOC} as in Fig. 4, right). This result, which simplifies understanding of the effect of perforations, seems to contradict some conceptions of the TM-to-ossicular chain coupling mechanisms. For example, this result indicates that interruption of a sizable fraction of TM radial fibers (e.g., as in Fig. 1, right) may have little effect on TM-coupling function. To demonstrate larger effects of changes in TM integrity, a structural modification was designed to disconnect more extensively the TM from the manubrium (handle) of the malleus, while minimizing changes in the pressure difference across the TM. In other words, in contrast to the perforations, this modification might produce only small changes in the pressure difference across the TM ($H_{\Delta TM}$) while dramatically changing the coupling H_{TOC} .

In one ear, we slit the TM with a myringotomy knife along the manubrium of the malleus in four stages as schematized in Fig. 7. Each slit completely penetrated the TM, as it was possible to view the middle-ear cavity through the slit.

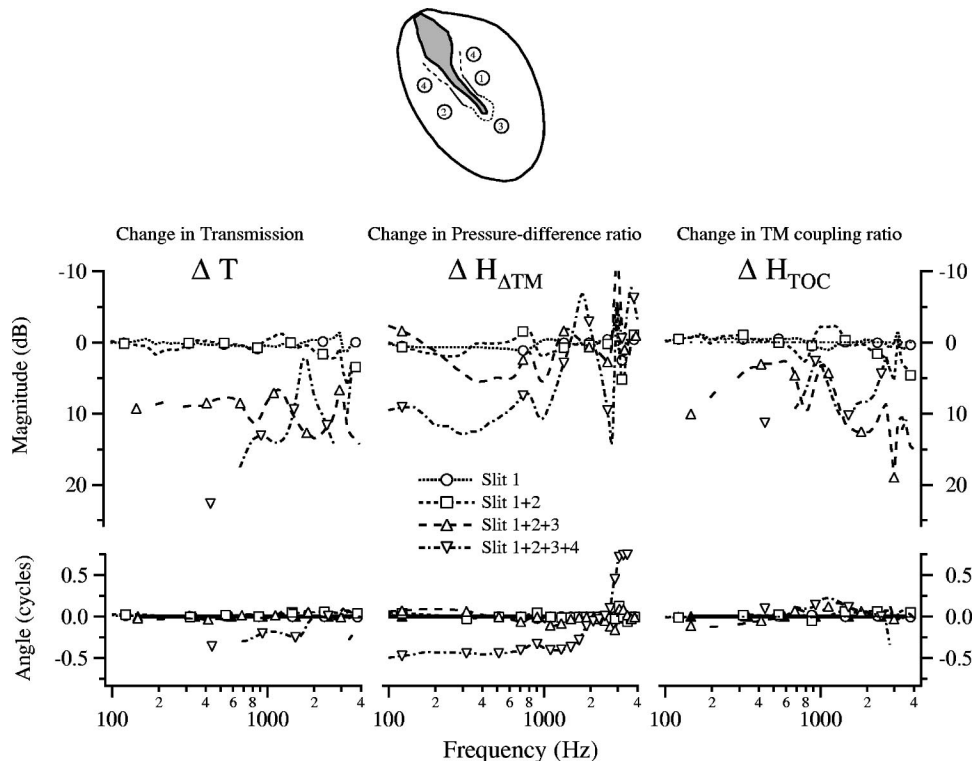


FIG. 7. Change in V_S/P_{TM} (left), $H_{\Delta TM}$ (center), and H_{TOC} with slit configuration the parameter; changes are defined as the ratio between the normal measurement and the perforated measurement (i.e., norm/perf) with [norm/perf] plotted in dB with positive down so that these plots have the format of standard audiograms. The slit configuration is schematized in the center of the figure. Slit 1, indicated by a solid line, was made first along the posterior edge of the manubrium of the malleus. Slit 1 was about 2 mm long. Next slit 2, also about 2 mm long and indicated by a solid line, was made along the anterior border of the manubrium. Next, slit 3, indicated by a dashed line, was made to connect slits 1 and 2 around the distal end of the manubrium (umbo). Finally, slit 4, with two components, was made so that the combined slit encompassed the perimeter of the manubrium and extended approximately to the lateral process of the malleus. Symbols are plotted at every eighth data point for V_S/P_{TM} and H_{TOC} and every 25th data point for $H_{\Delta TM}$. "Gaps" between V_S/P_{TM} data points result when measurements at some frequencies are excluded as a result of the mechanical artifact; these exclusions generally occur when the reduction in stapes velocity is large.

Figure 7 shows changes in measurements made with four slit conditions. First, consider the single 2 mm slit along the posterior part of the manubrium (labeled slit 1). The left column of Fig. 7 indicates that there was no change in T from normal with this first slit. This slit certainly penetrated the TM, but after the slit was made the margins of the slit were observed under a microscope to be bridged by moisture. Figure 7 (center column) shows that slit 1 did not affect the pressure-difference ratio ($H_{\Delta TM}$) either. Similar to slit 1, slit 2 was also self sealing with moisture and the responses with slit 2 added were similar to those with slit 1 only: neither T nor $H_{\Delta TM}$ changed much from normal (<2 dB in magnitude).

Larger changes in T and $H_{\Delta TM}$ occurred with the addition of slits 3 and 4, in which the slits were longer and remained open over their entire length. With the addition of slit 3, the change in $|T|$ is relatively flat below 1000 Hz at about 10 dB, and with the addition of slit 4 the change is between 10 and 25 dB and has some variation with frequency. Examination of the second and third columns of Fig. 7 shows that for the longer third and fourth configurations, changes in $|H_{\Delta TM}|$ increase to up to 10 dB for frequencies from 400 to 2000 Hz, and changes in $|H_{TOC}|$ can approach 10–20 dB at some frequencies. Measurements of T below 400 are not available because of the mechanical artifact, and it is possible that changes in $|H_{TOC}|$ could greatly exceed 20 dB at these lower frequencies. Even though changes in H_{TOC} are larger than with our circular perforations, the changes of only 10–20 dB at higher frequencies in configuration 4 seem inconsistent with the extensive disruption of the manubrium's attachment to the TM. In summary, this experiment suggests that major interruption of the TM structure near the manubrium has only moderate effects (i.e., <20 dB) on H_{TOC} for frequencies greater than 400 Hz.

IV. DISCUSSION

A. Comparison to other work

1. Frequency dependence of loss with perforations

Our measurements of perforation-induced changes in transmission show a clear frequency dependence; Fig. 4 shows that for all perforation sizes, the transmission changes are greatest at the lowest frequency and decrease toward zero as frequency increases toward 1000–2000 Hz. There can be increases (up to 20 dB) in transmission in the 1000–2000 Hz region. Above 2000 Hz, the losses are typically less than 10 dB. (We note that our largest perforations covered 50% of the TM; larger perforations could produce different loss characteristics.)

These results are consistent with the cat cochlear-potential measurements of McArdle and Tonndorf (1968) and Kruger and Tonndorf (1977,1978) (Fig. 8), and the umbo-velocity measurements of Bigelow *et al.* (1996) in rat, in all of which perforations in the TM produced their largest effects at the lowest frequencies. Similarly, the temporal-bone measurements of Nishihara *et al.* (1993) and the audiometric results of both Tavin *et al.* (1988) and Rosowski *et al.* (1996) show that tympanostomy tubes in the TM produced their largest losses at the lowest frequencies. The perforation-

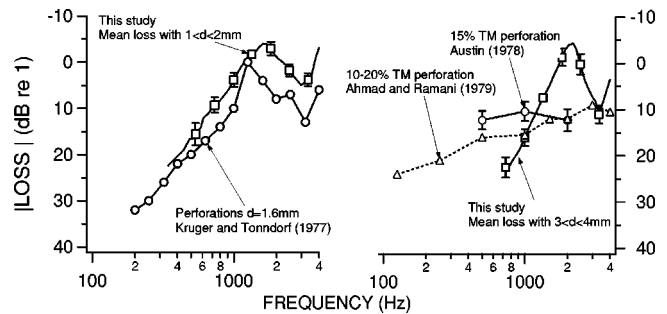


FIG. 8. Comparison of our mean change in transmission (i.e., “loss”) to measurements of transmission loss from Kruger and Tonndorf (1977) and Austin (1978). Left: Comparison of results of Kruger and Tonndorf (1977) to our mean transmission change (ΔT) with perforations of diameter d such that $1 < d \leq 2$ mm (taken from Fig. 4). The perforation diameter of the Kruger and Tonndorf (1977) measurements was $d = 1.6$ mm, and their loss measurements were from cat cochlear potential data. Right: Comparison of audiologic data from Austin (1978) with perforations that covered about 15% of the TM (about 3.4 mm in diameter) and perforations from Ahmad and Ramani that covered 10%–20% of the TM. Here, we plot our mean ΔT with perforation diameters d such that $3 < d \leq 4$ mm.

induced loss was most prominent at the lowest frequencies and the loss decreased with increasing frequency in the audiometric data of Ahmad and Ramani (1979) (Fig. 8). Our measurements show increases in sensitivity in the 2000 Hz region that are not found in the average of the measurements of Ahmad and Ramani (1979); this difference may result from variations in middle-ear cavity volume (Voss *et al.*, 2001d). In our population of ears, the volumes were very similar for all ears and thus the resonant frequency between the acoustic mass of the perforation and the acoustic compliance of the middle-ear cavity would be similar for perforations of the same size. In a clinical population, however, larger variations in middle-ear cavity volume are likely (Molvaer *et al.*, 1978), and thus this resonant frequency where sensitivity is increased, would not be the same across ears. As a result, averaging audiograms from a clinical population would tend to obscure the region of the increased sensitivities.

Our results disagree with results of Békésy (1936) in human, measurements of Payne and Githler (1951) in cat, and the audiologic data of Austin (1978) (Fig. 8). Using a temporal-bone preparation, Békésy (1936) found no differences in the motion of the malleus with a normal TM and a 0.6-mm-diam perforation for frequencies above 400 Hz, although below 100 Hz he did find a reduction in motion that increased inversely with frequency. However, if Békésy's perforations were effectively closed by moisture on the TM, as happened with our slit experiments (Fig. 7), then his measurements are consistent with our results. Békésy also investigated the effect of a “lens-shaped tear” of the TM [“extending from the end of the manubrium to one edge and having a width of 2 mm”] on a living human subject (Békésy, 1936). In this case, hearing in the contralateral ear was compared to hearing in the ear with the perforation, and Békésy concluded that the perforation “had no noticeable effect on thresholds from 50 to 4000 cps [Hz] except to alter slightly the small deviation in the frequency function.” As no further details are given, it is difficult to explain the clear

difference between this observation and our results.

Payne and Githler (1951) measured a reduction in cochlear potential that increased with perforation size, and they found these reductions were nearly frequency independent. McArdle and Tonndorf (1968) showed that the Payne and Githler (1951) results have a serious methodological problem. In the Payne and Githler study, the middle-ear cavity was opened to surrounding space. The open cavity caused the pressure on the middle-ear side of the TM to be smaller than it would have been with an intact middle-ear cavity, thus increasing the pressure difference across the TM and decreasing the effect of the perforation on the pressure difference across the TM.

Austin (1978) describes the frequency-dependence of loss with perforation size as: “the presence of a perforation does not significantly affect the frequency response of the middle ear, since a flat hearing loss was observed for the three frequencies studied as well as for each size of perforation” (Austin, 1978, p. 372). Indeed, the means of audiograms at 500, 1000, and 2000 Hz that Austin (1978) presents do not show appreciable frequency dependence. However, our measurements with perforation sizes similar to Austin’s sizes show a clear frequency dependence (Fig. 8, right). One hypothesis for the differences between our measurements and Austin’s audiograms is that errors occur with audiograms measured in ears with perforations (Voss *et al.*, 2000a, e). Because the perforated ear’s impedance may be substantially lower than a normal ear, audiometric earphones can generate a lower-than-normal sound-pressure level when they are coupled to a perforated ear. This lower-than-expected sound-pressure level results in audiograms that make the hearing loss at the lower frequencies appear larger than they actually are. If such an error affects Austin’s audiograms, the “corrected” audiograms would have smaller loss at low frequencies and the difference between Austin’s audiometric results and our measurements would be even greater than that shown in Fig. 8 (right). Thus, the possibility that errors occurred in the ear-canal pressures generated during audiometry does not seem to account for the differences between Austin’s data and ours. We have no explanation for the differences.

2. Effect of perforation size on transmission

Many studies of perforations, both animal and clinical studies, show that loss increases as perforation size increases (e.g., Anthony and Harrison, 1972; Austin, 1978; Ahmad and Ramani, 1979; Bigelow *et al.*, 1996). Our measurements show that perforation size has a big effect, and that for each perforation size, the perforation-induced transmission change can be described efficiently in three frequency regions. First, for the lowest frequencies, as perforation size increases, the loss (i.e., change from normal in transmission) increases monotonically and the slope of the loss magnitude versus frequency is about 40 dB per decade. Second, for “middle-frequencies,” the loss is near zero or slightly negative, and the frequency of this increased transmission increases with perforation size. The limits of the “middle-frequencies” range depend on and increase monotonically with perforation size. Third, for frequencies above 2000 Hz, the larger perfo-

ration sizes show the larger deviations from zero; both the gains and the losses increase with perforation size and can approach 10 dB. Thus, strictly speaking, loss increases monotonically with perforation size only in the low-frequency region.

3. Effect of perforation location on transmission

The results presented here are from perforations made in both the anterior-inferior and the posterior-inferior quadrants of the TM. We analyzed our results to determine if the perforation location plays an important role in the perforation-induced changes in stapes velocity. These comparisons are presented in detail elsewhere (Voss, 1998; Voss *et al.*, 2000c); the main conclusion is that changes in stapes velocity (i.e., transmission) do not appear to depend on perforation location in our temporal-bone preparation, with the kinds of perforation illustrated in Fig. 1.

This result contradicts the widely held clinical view that a posterior-inferior perforation results in larger hearing loss than an anterior-inferior perforation (e.g., Schuknecht, 1993b, p. 196; Glasscock and Shambaugh, 1990, p. 314; Pickles, 1987, pp. 60–61). The usual explanation for the location dependence is that a posterior perforation is closer to the round window, and as a result the pressure acting at the round window “cancels” the cochlear response more than the round-window pressure associated with perforations at other locations. Voss (1998, Chap. 3) used measurements of the oval and round window pressures with perforations at different locations to show that the perforation location has no effect on the pressure difference between the oval-window and the round-window pressures. Thus, our measurements reject both the view that loss depends on perforation location and the presumed theoretical basis.

Ahmad and Ramani (1979) investigate how the perforation locations of anterior-inferior versus posterior-inferior affect hearing levels. For their smaller perforations (<10% of the TM), they find hearing is independent of perforation location. With larger perforations, it appears that hearing levels are slightly more sensitive (i.e., lower) with anterior perforations; however, the difference between the locations is only for the lowest frequencies (<1000 Hz) and the differences appear small. In fact, it is not clear that there is a statistical difference between the locations, as no measures of intersubject variation are provided. Ahmad and Ramani (1979) conclude: “It is seen that the difference in hearing losses...between antero- and postero-inferior perforations, is appreciable only at the lowest frequencies. At other frequencies it is minimal; indeed, it [effects of location on hearing losses] is almost negligible for clinical purposes.” Thus, this study of audiograms, for a fairly large sample ($N=70$) of well-described perforations, provides, at best, weak support for the common clinical view.

B. Dominant loss mechanism: Change of pressure difference across the TM

Equation (4) expresses middle-ear sound transmission as the product of two ratios, representing the effects of (1) the pressure difference across the TM ($H_{\Delta TM}$) and (2) the cou-

pling of the pressure difference to the motion of the TM, ossicles, and cochlea (H_{TOC}). Our results show that perforation-induced changes in $H_{\Delta\text{TM}}$ are similar to perforation-induced changes in stapes velocity (Fig. 4), while perforation-induced changes in H_{TOC} are generally smaller than changes in either stapes velocity or $H_{\Delta\text{TM}}$ (i.e., Fig. 4). Thus, we conclude that (1) the dominant mechanism for changes in sound transmission is a perforation-induced change in the pressure difference across the TM, and (2) changes in the mechanical linkage of the TM and ossicles to the cochlea make secondary contributions to the total transmission changes.

C. Dependence of TM function on its structural integrity

A main result of this paper is that perforations do not alter (much) the coupling of the pressure difference across the TM to ossicular motion (i.e., H_{TOC}). Some basic questions arise concerning the processes involved. For example, if the TM's coupling of force to the manubrium occurs at the umbo and/or along the length of the manubrium (e.g., Dallos, 1973, Fig. 3.4; Wever and Lawrence, 1954, pp. 90–114), how can (1) the removal of the TM from around much of the umbo (Fig. 1), and (2) extensive slits along the margins of the manubrium (Fig. 7) have only a small effect on H_{TOC} (for frequencies above 400 Hz)? Perhaps the coupling between the peripheral region of the TM through the superior part of the manubrium is of primary importance. Perhaps fluid filling a slit couples the TM to the manubrium nearly as well as the TM itself. In this case the microstructure of the TM seems unimportant to its function. This idea is consistent with clinical practice of reconstructing TMs with a variety of materials as well as the observation that the eardrums of normal-hearing ears can have tympanosclerotic plaques or be abnormally thinned as a result of past disease (Hunter, 1993). In general, the results of this one experiment suggest that further experimental investigation is needed to determine the importance of TM structural and mechanical features for its function.

D. Clinical application of results

Our results describe hearing loss caused by different sized perforations in otherwise normal ears. These results should aid clinicians in determining whether a specific hearing loss results only from a perforation or whether other middle-ear pathology should be expected. The following features are consistent with a hearing loss from a perforation only: (1) losses that decrease as frequency increases up to about 1000 Hz, (2) losses or gains near zero in the 1000–2000 Hz range, and (3) for frequencies above 2000 Hz, losses that do not exceed about 10 dB for perforations that are less than 50% of the TM area. Some of these features may be difficult to distinguish on standard audiograms taken at only five or six octavespaced frequencies, but audiometric results in perforated ears that do not fit this pattern are suggestive of additional pathology.

The result that the dominant mechanism for transmission loss is a reduction in the pressure difference across the TM

provides experimental support for the well-known clinical “paper patch test” (Schuknecht, 1993a; Glasscock and Shambaugh, 1990).

“A patch of thin paper of appropriate size is coated on one surface with unguentum and placed over the perforation. Results of hearing tests before and after application of the paper patch provide a prediction of the functional outcome of surgery” (Schuknecht, 1993a, p. 5).

In the “paper patch test,” the patch returns the pressure difference across the TM to near normal levels. The patch does not return to normal any of the structural modifications made to the TM by the perforation (e.g., disruption of fibers or changes in tension). Thus, the observation that the “paper patch test” successfully improves hearing in many cases of perforated TMs is consistent with the results that show the pressure difference is the primary mechanism of hearing loss with perforations.

Even though numerous clinical studies have examined hearing levels with perforations, a clear picture of middle-ear function with perforations has not emerged. Instead, it is commonly observed that similar appearing perforations result in dramatically different hearing levels. For example,

“In general, the larger the perforation, the greater the hearing impairment, but this relationship is not constant and consistent in clinical practice; seemingly identical perforations in size and location produce different degrees of hearing loss. The reasons for the variations in the hearing effects of simple perforations are not easily defined” (Glasscock and Shambaugh, 1990, p. 337).

Some, if not all, of this variability may result from differences in middle-ear cavity air volumes. The theoretical treatment of the results (Voss *et al.*, 2001d) demonstrates that middle-ear function with perforations depends on the middle-ear cavity volume. Although Békésy (1936) alludes to the effect of the cavity volume, the relationship between hearing levels and middle-ear cavity volume has not previously been described quantitatively. We now have a theoretical structure that describes the interaction between the perforation and the cavity volume, and it appears that normal variations in cavity volume can lead to differences in low-frequency hearing levels of up to 20 dB in ears with otherwise similar perforations. Future clinical studies can test for the importance of middle-ear cavity volume by estimating this quantity via low-frequency impedance measurements and/or CT scans.

ACKNOWLEDGMENTS

This work was supported by training and research grants from the NIDCD. We thank Diane Jones of the Oto-Pathology Laboratory at the Massachusetts Eye and Ear Infirmary for obtaining temporal bones and Christopher Shera of the Eaton Peabody Laboratory at the Massachusetts Eye

and Ear Infirmary for helpful discussions. We also thank two JASA reviewers, Dr. Robert H. Margolis and an anonymous reviewer, for helpful suggestions.

- Ahmad, S. W., and Ramani, G. V. (1979). "Hearing loss in perforations of the tympanic membrane," *J. Laryngol. Otol.* **93**, 1091–1098.
- Allen, J. B. (1986). "Measurement of eardrum acoustic impedance," in *Peripheral Auditory Mechanisms*, edited by J. B. Allen, J. L. Hall, A. Hubbard, S. T. Neely, and A. Tubis (Springer, Berlin), pp. 44–51.
- Anthony, W. P., and Harrison, C. W. (1972). "Tympanic membrane perforations; effect on audiograms," *Arch. Otolaryngol.* **95**, 506–510.
- Austin, D. F. (1978). "Sound conduction of the diseased ear," *J. Laryngol. Otol.* **92**, 367–393.
- Békésy, G. v. (1936). "Zur Physik des Mittelohres and über das Hören bei fehlerhaftem Trommelfell," *Akust. Z.* **1**, 13–23 (English translation, pp. 104–115 in Békésy, 1960).
- Békésy, G. v. (1960). *Experiments in Hearing*, edited by E. G. Wever (McGraw-Hill, New York).
- Bigelow, D. C., Swanson, P. B., and Saunders, J. C. (1996). "The effect of tympanic membrane perforation size on umbo velocity in the rat," *Laryngoscope* **106**, 71–76.
- Bright, R. A., Moore, R. M., Jeng, L. L., Sharkness, C. M., Hamburger, S. E., and Hamilton, P. M. (1993). "The prevalence of tympanostomy tubes in children in the United States, 1988," *Am. J. Public Health* **83**, 1026–1028.
- Dallos, P. (1973). *The Auditory Periphery—Biophysics and Physiology* (Academic, New York).
- Egolf, D. (1977). "Mathematical modeling of a probe-tube microphone," *J. Acoust. Soc. Am.* **61**, 200–205.
- Glasscock, M. E., and Shambaugh, G. E. (1990). *Surgery of the Ear*, 4th ed. (Saunders, Philadelphia).
- Huang, G. T., Rosowski, J. J., Flandermeier, D. T., Lynch, T. J., and Peake, W. T. (1997). "The middle ear of a lion: Comparison of structure and function to domestic cat," *J. Acoust. Soc. Am.* **101**, 1532–1549.
- Hughes G. B. and Nodar, R. H. (1985). "Physiology of hearing," in *Textbook of Clinical Otolaryngology*, ed. by G. B. Hughes (Thieme-Strutton, Inc., New York), Chap. 7, pp. 71–77.
- Hunter, L. L. (1993). "Auditory sequelae of recurrent and persistent otitis media with effusion in children," Ph.D. thesis, University of Minnesota.
- Kruger, B., and Tonndorf, J. (1977). "Middle ear transmission in cats with experimentally induced tympanic membrane perforations," *J. Acoust. Soc. Am.* **61**, 126–132.
- Kruger, B., and Tonndorf, J. (1978). "Tympanic membrane perforations in cats: Configurations of losses with and without ear canal extensions," *J. Acoust. Soc. Am.* **63**, 436–441.
- Lim, D. (1970). "Human tympanic membrane an ultrastructural observation," *Acta Oto-Laryngol.* **70**, 176–186.
- Lynch, T. J., Peake, W. T., and Rosowski, J. J. (1994). "Measurements of the acoustic input impedance of cat ears: 10 Hz to 20 kHz," *J. Acoust. Soc. Am.* **96**, 2184–2209.
- McArdle, F. E., and Tonndorf, J. (1968). "Perforations of the tympanic membrane and their effects upon middle-ear transmission," *Arch. Ohren. Nasen Kehlkopfheilkd.* **192**, 145–162.
- Mehmke, V. S. (1962). "Der Hörverlust bei der Perforation des Trommelfelles," *Z. Laryngol. Rhinol. Otol.* **41**, 677–682.
- Møller, A. R. (1965). "An experimental study of the acoustic impedance of the middle ear and its transmission properties," *Acta Oto-Laryngol.* **60**, 129–149.
- Molvaer, O., Vallersnes, F., and Kringlebotn, M. (1978). "The size of the middle ear and the mastoid air cell," *Acta Oto-Laryngol.* **85**, 24–32.
- Nishihara, S., Aritomo, H., and Goode, R. L. (1993). "Effect of changes in mass on middle ear function," *Otolaryngol.-Head Neck Surg.* **109**, 899–910.
- Payne, M. C., and Githler, F. J. (1951). "Effects of perforations of the tympanic membrane on cochlear potentials," *Arch. Otolaryngol.* **54**, 666–674.
- Pickles, J. O. (1987). "Physiology of the ear," in *Scott-Brown's Otolaryngology: Basic Sciences*, edited by D. Wright (Butterworths, London), Vol. 1, Chap. 2, pp. 59–60.
- Rabinowitz, W. M. (1981). "Measurement of the acoustic input immittance of the human ear," *J. Acoust. Soc. Am.* **70**, 1025–1035.
- Ravicz, M. E., Rosowski, J. J., and Voigt, H. F. (1992). "Sound-power collection by the auditory periphery of the Mongolian gerbil *Meriones unguiculatus*. I. Middle-ear input impedance," *J. Acoust. Soc. Am.* **92**, 157–177.
- Rosowski, J. J., Merchant, S. N., Ravicz, M. E., Voss, S. E., Caradonna, D., Cunningham, M. J., and Peake, W. T. (1996). "Analysis of acoustic mechanisms in middle-ear pathology and reconstruction," in *Middle Ear Mechanics in Research and Otolaryngology*, edited by K.-B. Hüntenbrink (Dresden University of Technology, Dresden), pp. 183–190.
- Sadé, J. (1982). "Prologue," in *Proceedings of the Second International Conference of Cholesteatoma and Mastoid Surgery*, edited by J. Sadé (Kugler, Amsterdam), p. 1.
- Schuknecht, H. F. (1993a). "Office examination of the ear," in *Surgery of the Ear and Temporal Bone* (Raven, New York), Chap. 1, pp. 1–8.
- Schuknecht, H. F. (1993b). *Pathology of the Ear*, 2nd ed. (Lea & Febiger, Malvern, PA).
- Shambaugh, G. (1967). *Surgery of the Ear*, 2nd ed. (Saunders, Philadelphia).
- Shambaugh, G. E., and Glasscock, M. E. (1980). *Surgery of the Ear*, 3rd ed. (Saunders, Philadelphia).
- Tavin, M. E., Gordon, M., and Ruben, R. J. (1988). "Hearing results with the use of different tympanostomy tubes: A prospective study," *Int. J. Pediatric Otorhinolaryngology* **15**, 39–50.
- Terkildsen, K. (1976). "Pathologies and their effect on middle ear function," in *Acoustic Impedance and Admittance. The Measurement of Middle Ear Function*, edited by A. S. Feldman and M. A. Wilber (The Williams and Wilkins Company, Baltimore), pp. 78–102.
- Voss, S. E. (1998). "Effects of tympanic-membrane perforations on middle-ear sound transmission: measurements, mechanisms, and models," Ph.D. thesis, Massachusetts Institute of Technology.
- Voss, S. E., Rosowski, J. J., Merchant, S. N., and Peake, W. T. (2000b). "Acoustic responses of the human middle ear," *Hear. Res.* **150**, 43–69.
- Voss, S. E., Rosowski, J. J., Merchant, S. N., and Peake, W. T. (2000c). "How do tympanic-membrane perforations affect human middle-ear sound transmission?" *Acta Oto-Laryngologica* (in press).
- Voss, S. E., Rosowski, J. J., Merchant, S. N., and Peake, W. T. (2001d). "Middle-ear function with tympanic-membrane perforations. II. A simple model," *J. Acoust. Soc. Am.* **110**, 1445–1452.
- Voss, S. E., Rosowski, J. J., Merchant, S. N., Thornton, A. R., Shera, C. A., and Peake, W. T. (2000e). "Middle ear pathology can affect the ear-canal sound pressure generated by audiologic earphones," *Ear Hear.* **21**, 265–274.
- Voss, S. E., Rosowski, J. J., and Peake, W. T. (1996). "Is the pressure difference between the oval and round windows the effective acoustic stimulus for the cochlea?," *J. Acoust. Soc. Am.* **100**, 1602–1616.
- Voss, S. E., Rosowski, J. J., Shera, C. A., and Peake, W. T. (2000a). "Acoustic mechanisms that determine the ear-canal sound pressures generated by earphones," *J. Acoust. Soc. Am.* **107**, 1548–1565.
- Wever, E. G., and Lawrence, M. (1954). *Physiological Acoustics* (Princeton University Press, Princeton).